INORGANIC CHEMISTRY
FRONTIERS

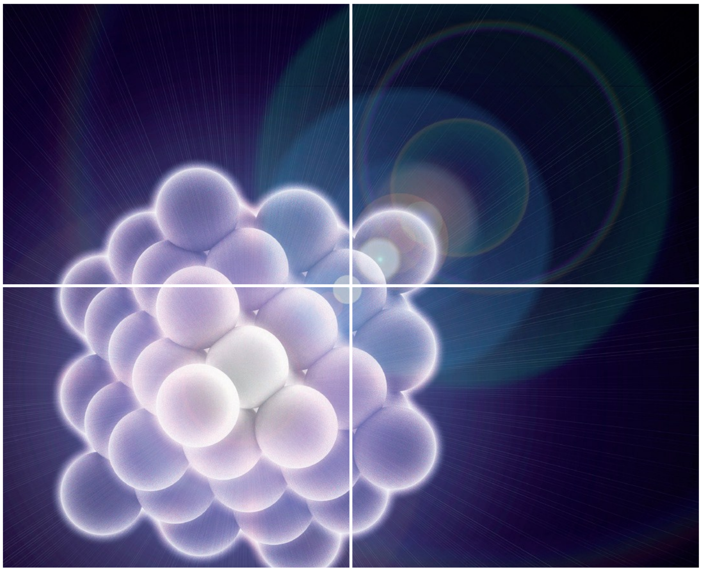

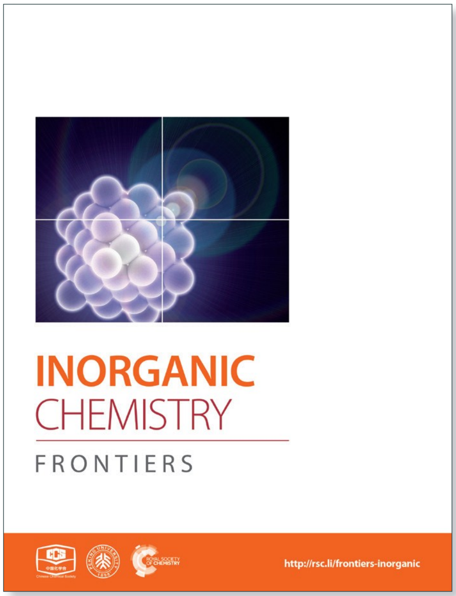

Journal Name

RSCPublishing

ARTICLE

Bimetallic layer-by-layer films and their application in catalytic hydrogenation of olefin

Cite this: DOI: 10.1039/x0xx00000x

Shuiying Gao,[a] Weijin Li,[a] Rong Cao*[a]

Received 00th January 2015,
Accepted 00th January 2015

DOI: 10.1039/x0xx00000x

www.rsc.org/

Since bimetallic catalysts exhibit enhanced activity and stability over their monometallic counterparts, bimetallic film catalysts $(Pd/bpy/Pt/bpy)_n$, were first prepared by alternating immersions of a substrate in K_2PdCl_4 precursor (or K_2PtCl_4 precursor) and bpy (bpy = 4, 4'-bipyridyl) solutions through layer-by-layer (LbL) self-assembly method. The self-assembly of bimetallic films was characterized by UV-vis spectra. The absorbance increases with the number of bilayers and the film growth shows a good linear correlation between the optical absorption and the number of $(Pd/bpy/Pt/bpy)_n$. Pd and Pt content of $(Pd/bpy/Pt/bpy)_5$ films were determined by 2.0×10^{-7} and 8.4×10^{-8} mol through inductively coupled plasma OES spectrometer (ICP-OES), respectively. The as-prepared $(Pd/bpy/Pt/bpy)_5$ film demonstrates a remarkable catalytic activity toward hydrogenation of olefin bearing different characters under mild conditions. The relationship between the catalytic activity and the number of bilayers was investigated. The catalytic activity of the $(Pd/bpy/Pt/bpy)_n$ films increases with the number of bilayers below 4 bilayers for styrene hydrogenation and remains unchanged after 4 bilayers. X-ray photoelectron spectroscopy (XPS) and transmission electron microscopy (TEM) illustrate that Pd and Pt ions of $(Pd/bpy/Pt/bpy)_n$ films are *in situ* reduced into Pd and Pt nanoparticles (NPs) during the hydrogenation process, resulting in high catalytic activity. In addition, the control experiments show that the catalytic activity of our bimetallic catalysts is higher than that of the prereduced bimetallic catalyst and the physical mixtures of the Pd and Pt film catalysts. As compared to traditional heterogeneous catalysts, the film catalysts have superior advantages of easy separation and good recyclability, because they are easily removed from the reaction mixture without separation filtration.

1. Introduction

Research interest in bimetallic catalysts has drawn wide attention.[1, 2] Bimetallic catalysts, due to their tunable chemical/physical properties, exhibit unique properties which are distinct from those of their monometallic counterparts. Thus, bimetallic catalysts exhibit enhanced selectivity, activity, and stability over traditional monometallic ones.[3, 4] Synthetic strategies of bimetallic catalysts, including wet chemical approach, electrochemical synthesis, and thermal reduction, have been carried out in liquid mixtures or solutions. Besides, the layer-by-layer (LbL) technology, due to its simplicity, robustness, and versatility, offered an important method for bimetallic catalysts. The LbL technology has become a popular technique for thin film preparation.[5-8] Compared to thin film deposition methods such as physical vapor deposition and chemical vapor deposition, LbL method is extremely simple and cheap. As compared to traditional heterogeneous catalysts, films-based catalysts are easily removed from the reaction mixture without separation filtration.[9] To our knowledge, there are many reports on monometallic Pd films using polyelectrolytes as building blocks.[10-14] In general, polyelectrolyte multilayers have been explored as matrices for synthesis of zero-charge nanoparticle (NPs) in order to generate large surface area heterogeneous catalyst, such as LbL PAA/PEI-Pd(0) and Pd/PVP films (PAA =poly(acrylic acid, PEI =polyethylenimine, PVP =poly(4-vinylpyridine)). Monometallic Pd films were loaded within LbL multilayers by alternate adsorption of palladium ion and pyridyl ligand layers onto solid slides.[15-20] By comparison, the bimetallic films have been rarely reported. To date, only bimetallic gold-silver (Au-Ag) nanoparticles were synthesized by LbL polyelectrolyte multilayer (PEM) nanoreactors.[21-24] No matter monometallic or bimetallic LbL films, polyelectrolytes are generally ulitized as buliding blocks forming NPs and small molecules are rarely used as buliding blocks. Moreover, *in situ* synthesis strategy of bimetallic catalysts within the LbL films were also rarely reported. The *in situ* LbL strategy nanoreactor possesses several distinct advantages, such as tunable structure and composition and good chemical stability. More importantly, the *in situ* LbL synthesis strategy combines the synthesis and immobilization within one step, for practical applications such as sensor and catalysis.[23]

The noble metals such as Pd and Pt are widely used in hydrogenation reaction that is significant in petroleum refining industry. Based on metal ion-ligand interaction, small organic functional ligands can be used as building blocks to construct LbL Pd/Pt bimetallic self-assembly films. Each metal ion is separated and connected by organic ligands. Since bimetallic catalysts exhibit enhanced activity, Pd/Pt bimetallic-pyridyl catalytic film for catalytic hydrogenation reactions was investigated (Scheme 1). The Pd/Pt bimetallic-pyridyl catalytic films exhibited a remarkable catalytic activity over monometallic ones. The catalytic films are not desorbed from slides and have good recyclability. The process of the metal ions *in situ* reduced into NPs was discussed through X-ray photoelectron spectroscopy (XPS) and transmission electron microscopy (TEM).

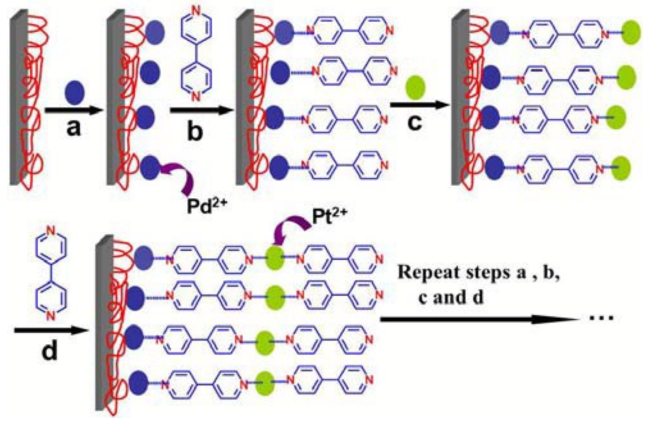

Scheme 1 The self-assembly process of (Pd/bpy/Pt/bpy)$_n$ films.

Experimental section

Instrument

UV-vis absorption spectra were recorded on a quartz slide with a Lambda35 spectrophotometer (Perkin-Elmer, USA). Analysis of noble metal content was measured by inductively coupled plasma OES spectrometer (ICP-OES) (Ultima2, France). Gas chromatography (GC) was performed on Agilent 7890A (USA). High-resolution X-ray photoelectron spectra (XPS) were collected at a takeoff angle of 45° using PHI Quantum 2000 scanning ESCA microprobe (Physical Electronics, USA) with an Alα X-ray line (1486.6 eV). Transmission electron microscopy (TEM) was generated on a JEM-2010 operated at 120 kV. Small pieces of a multilayer film were scraped off the quartz substrate in ethanol and transferred to a copper grid.

Layer-by-layer assembly (Pd/bpy/Pt/bpy)$_n$ multilayer films

The preparation of (Pd/bpy/Pt/bpy)$_n$ multilayer films are as follows: The quartz slides (size 25 mm × 12 mm × 1 mm) were cleaned with a “piranha solution” at 80 ℃ for 40 min, and thoroughly rinsed with water. Further purification was carried out by immersion in an H_2O-H_2O_2-NH_3OH (5:1:1) (V/V/V) bath for 30 min at 70 ℃. The clean slides were first immersed in PEI solution for 20 min. The slides pre-coated with poly(ethylenimine) (PEI) were alternately immersed in K_2PdCl_4 aqueous solution (5 mM, 10 mL), bpy (5 mM, 10 mL) ethanol solution, K_2PtCl_4 aqueous solution (5 mM, 10 mL) and bpy (5 mM, 10 mL) ethanol solution for 30 min. The substrates were washed with water and dried with nitrogen stream after each immersion. By repeating the above procedure, (Pd/bpy/Pt/bpy)$_n$ multilayer films were prepared and the self-assembly process was shown in Scheme 1.

Analysis of Pd and Pt content in (Pd/bpy/Pt/bpy)$_5$ multilayers

The quartz slide coated with (Pd/bpy/Pt/bpy)$_5$ was dissolved by aqua regia (10 ml). The content of Pd and Pt was determined by inductively coupled plasma OES spectrometer (ICP-OES).

Typical procedures for the hydrogenation of olefin

Hydrogenation reactions were carried out in a hydrogen atmosphere (1.2 atm) at 34 ℃. Typically, olefin (0.5 mmol), absolute ethanol (10 ml) and the quartz slide coated with (Pd/bpy/Pt/bpy)$_5$ film were added to the tube. The tube was sealed with a Teflon cap and evacuated and backfilled with H_2 three times. The mixture was stirred at a constant stirring speed (500 r/min) in the tube under an H_2 atmosphere. The conversion and yield were determined by GC analysis.

2. Results and Discussion

Preparation and characterization

The self-assembly of bimetallic films is based on the coordination bond between metal ions and the two terminal pyridyl groups of bpy. The self-assembly process is shown in Scheme **1**. As shown in Scheme **1**, The Pd^{2+} or Pt^{2+} ions were connected with bpy molecules. Palladium ions form the coordination bond with the terminal pyridyl group of bpy, whereas Pt ions form the coordination bond with the other pyridyl groups of bpy. The two coordination interactions constitute the films. In order to demonstrate the coordination interaction, UV-vis spectra of the solutions of metal precursors and bpy were performed (shown in Fig. S1, see ESI). The band of the bpy molecules occurs at 240 nm (Fig.S1a). The band at 233 nm is assigned to a ligend-to-metal charge transfer transition (LMCT) of the complex $PdCl_4^{2-}$ (Fig.S1b), while the band at 227 nm is assigned to LMCT of the complex $PtCl_4^{2-}$

(Fig.S1d). When the $PdCl_4^{2-}$ solution is mixed with the equimolar bpy molecules, two broad peaks at 244 nm and 273 nm occur (Fig.S1c). Similarly, the $PtCl_4^{2-}$ solution is mixed with the equimolar bpy molecules, two peaks are at 235 nm and 265 nm, respectively (Fig.S1e). Obviously, compared with individual metal precursor, the peak shape and position of mixture has been greatly changed and these peaks are red-shifted. Therefore, there exist coordination interaction between Pd and Pt ions and the terminal pyridyl group of bpy.

On this basis, the bimetallic-pyridyl $(Pd/bpy/Pt/bpy)_n$ films were prepared. UV-vis spectra also demonstrate the self-assembly process. The absorbance increases with the number of bilayers (Figure 1). The absorbance is from bpy ligand layer. The relationship between absorbance and the number of bilayers is shown in Figure 1b. The absorbance increases with the number of the outer layer of Pd/bpy or Pt/bpy. The film growth shows a good linear correlation with $R^2 = 0.9965$ (R^2 is a statistical calculation used with linear regressions) between the optical absorption at $\lambda_{max} = 278$ nm and the number of $(Pd/bpy/Pt/bpy)_n$, suggesting that bpy is incorporated into the films with a regular growth.

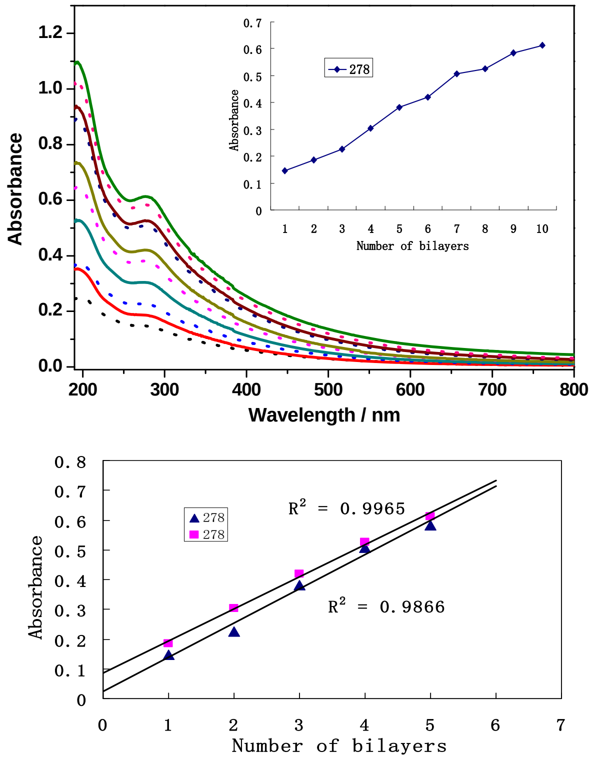

Fig.1 UV-vis spectra of $(Pd/bpy/Pt/bpy)_n$ films (a) and the relationship between absorbance and the number of bilayers (b). The dashed lines or triangle represent the outer layer of Pd/bpy; The solid lines or square represent the outer layer of Pt/bpy.

Catalytic performance of films for the olefin hydrogenation

The relationship between the substrate conversion and the number of $(Pd/bpy/Pt/bpy)_n$ bilayers was investigated. The catalytic activity of the films increases with the number of bilayers (as shown in Figure 2). However, when the number of $(Pd/bpy/Pt/bpy)_n$ bilayers reaches 5, the catalytic activity is not greatly improved and remains similar to 4 bilayers. This indicates that the activity is also related to the NPs of films. After 4 bilayers, thicker LbL films produce lower quality of NPs.

To explore the generality of the catalytic system, olefins bearing different characters were tested. The results are summarized in Table 1. For example, nitrobenzene is reduced into aniline (Table 1, entry 2), 3,7-dimethyl-1,6-octadien-3-ol is selectively hydrogenated to 3,7-dimethyl-6-octen-3-ol (Table 1, entry 4), and benzalacetone is selectively hydrogenated to benzylacetone (Table 1, entry 5). Moreover, for cyclohexene hydrogenation, bimetallic-pyridyl film $(Pd/bpy/Pt/bpy)_5$ gave good yield in 3.6 h (Table 1, entry 8), while monometallic $(Pd/bpy)_{10}$ film catalysts gave good yield in 8.0 h.[25] For other olefin substrates such as 3,7-dimethyl-1,6-octadien-3-ol and ethyl cinnamate, $(Pd/bpy/Pt/bpy)_5$ have high catalytic activity than the corresponding monometallic $(Pd/bpy)_{10}$ film catalysts.[25] Although Pt has catalytic activity in olefin hydrogenation, monometallic $(Pt/bpy)_{10}$ film catalysts exhibited lower catalytic activity for styrene or no activity for other olefin hydrogenation. Pd and Pt content of $(Pd/bpy/Pt/bpy)_5$ films were determined by 2.0×10^{-7} and 8.4×10^{-8} mol, respectively. Turnover number (TON) (moles of substrate converted per mole of catalyst) is calculated by 1760, which is higher than that of monometallic film $(Pd/bpy)_{10}$ in previous reports (TON: 1190).[24] Therefore, bimetallic-pyridyl film $(Pd/bpy/Pt/bpy)_5$ exhibits much better catalytic efficiency than monometallic $(Pd/bpy)_{10}$ film catalysts in previous report.[25]

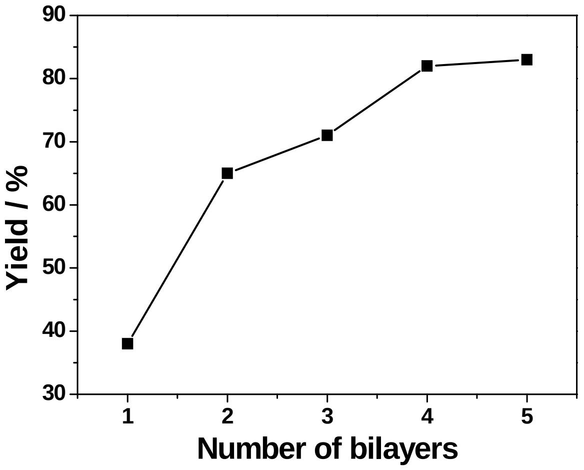

Fig.2 Relationship between styrene conversion and the number of $(Pd/bpy/Pt/bpy)_n$ bilayers during the 30 min reaction time.

Table 1 Hydrogenation of olefin and nitrobenzene over film catalysts

entry	Substrate	Product	Time	Yield (%) ^{a}
1	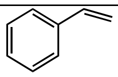	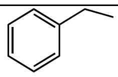	0.6 h	＞99
2	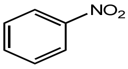	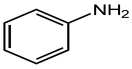	2.6 h	＞99
3	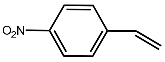	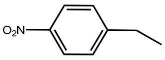	6 h	86
4	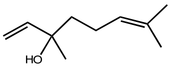	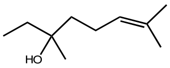	2 h	96
5	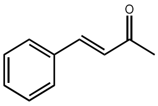	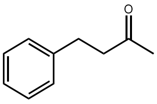	4.4 h	94
6	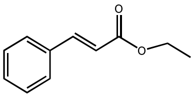	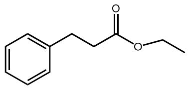	4.3 h	＞99
7	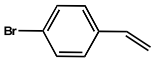	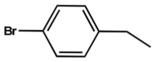	1.5 h	＞99
8	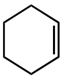	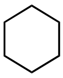	3.6 h	＞99

Reaction conditions: substrate (0.5 mmol), absolute ethanol (10 ml), Catalysts: (Pd/bpy/Pt/bpy)$_5$, stirring, H_2 (1.2 atm), 34℃. ^{a} Determined by GC methods.

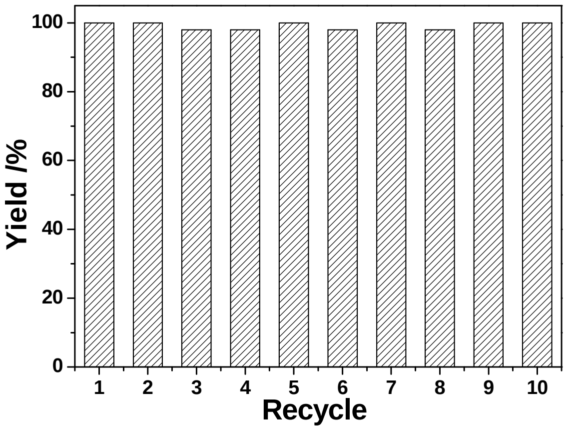

Fig.3 Recycling of (Pd/bpy/Pt/bpy)$_5$ films for 10 runs of styrene hydrogenation for 40 min.

To ensure that the immobilized NPs in the films represent the catalytically active species rather than soluble species leaching from film during the reaction process. A hot filtration test was performed. The (Pd/bpy/Pt/bpy)$_5$ catalysts were removed after 1 h for the nitrobenzene hydrogenation reaction and the reaction mixtures were kept to react for an additional 2 h under identical reaction conditions, no changes in conversion were observed. ICP analysis of the final reaction mixture shows that Pd and Pt concentrations are 0.056 ppm and 0.075 ppm, respectively, indicating metal leaching is negligible during the catalytic reaction. These results demonstrate the reaction proceeds in a heterogeneous fashion.

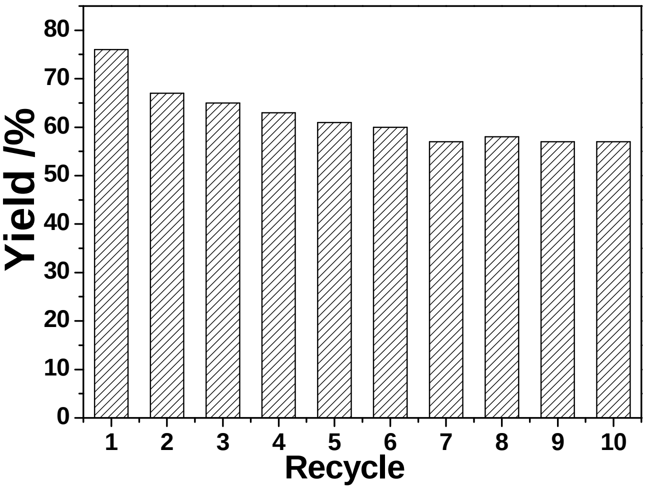

Fig.4 Recycling of (Pd/bpy/Pt/bpy)$_5$ films for 10 runs of nitrobenzene hydrogenation for 2 h.

The recycling of (Pd/bpy/Pt/bpy)$_5$ films was investigated. After completion of a catalytic reaction, solid glass slides modified with (Pd/bpy/Pt/bpy)$_5$ films were simply removed from the product, washed with ethanol, dried, and then reused in another catalytic cycle. This process was repeated for at least 10 cycles for the hydrogenation of styrene for 40 min and the yield of product remains over 95% (Figure 3). For nitrobenzene hydrogenation (Figure 4), the yield of aniline is 76% for 2 h in the first catalytic cycle and the yield is decreased to 67% in the second cycle. The higher activity is due to *in situ* reduced (Pd/bpy/Pt/bpy)$_5$ film catalyst in the first cycle. However, in other catalytic cycle, the obvious decrease of the catalytic activity did not occur and the yield remains stable. The number of cycles also reaches 10 cycles. Therefore, the results show that our film catalysts have good recyclability. Moreover, the recyling is more convenient as compared to the traditional heterogeneous catalysts, because they are easily removed from the reaction mixture without separation filtration.

The catalytic process was investigated by TEM and XPS. During the process of olefin hydrogenation, hydrogen gas was used as a reductant for metal ions besides hydrogen source for the hydrogenation reactions. XPS is recorded for the catalytic film after catalytic reduction. As shown in Figure 5, the peak position and intensity for the metal elements largely changes before and after the hydrogen reduction. Firstly, before the hydrogenation reaction, Pd ions are Pd(II) ions with the binding energy 337.4/342.4 eV, whereas the binding energy 72.8/76.0 eV corresponds to Pt(II) ions. After the 10th cycle of nitrobenzene hydrogenation, a couple of new peaks at 335.3/340.5 eV with high intensity are ascribed to Pd(0) (Figure 5a), which indicate that Pd(II) ions are reduced to Pd(0).[26] Meanwhile, a couple of new peaks at 71.5/74.7 eV occur with high intensity (Figure 5b), which corresponds to Pt(0).[27] During the process of styrene reduction, XPS also demonstrates the similar behaviors (Figure 6). Most of Pd(II) ions with the binding energy 337.4/342.4 eV are reduced into Pd(0) states (335.3/340.5 eV), while less than half of Pt(II) ions (72.8/76.0 eV) are reduced into Pt(0) states (71.5/74.7 eV) (Figure 6). As seen from the peak intensity, Pd(II) ions are more easily reduced than Pt(II) ions under the same condition, because the peak intensity of Pt(II) ions is stronger than that of Pd(II) ions after reduction. These results indicates that metal ions are bivalent metal ions before olefin hydrogenation, but metal ions are in the presence of mixed valences metal(II) and meta(0) with the hydrogenation carried through or increasing the number of cycles. Finally, all metal ions are reduced into NPs.

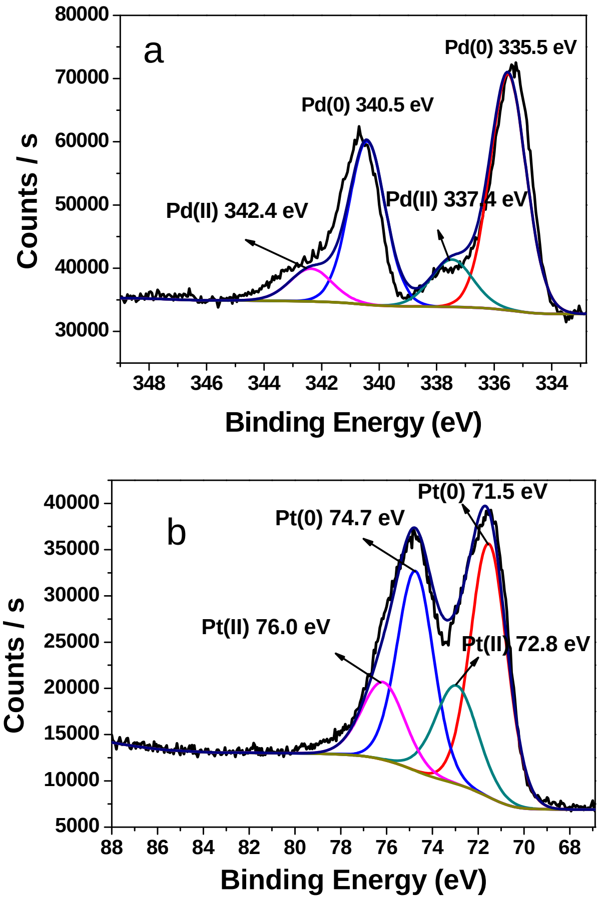

Fig.5 XPS spectra of the Pd3d (a) and Pt4f (b) region for $(Pd/bpy/Pt/bpy)_5$ film deposited on the solid glass substrate after the 10th cycle of nitrobenzene hydrogenation

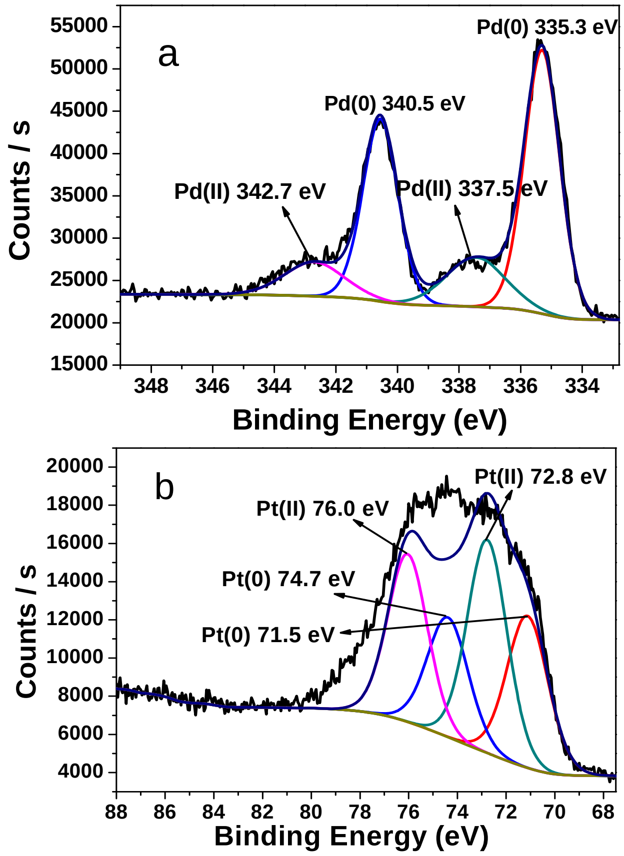

Fig.6 XPS spectra of the Pd_{3d} (a) and Pt_{4f} (b) region for $(Pd/bpy/Pt/bpy)_5$ film deposited on the solid glass substrate after the 10th cycle of styrene hydrogenation.

As shown in TEM images, the dispersion of particles in $(Pd/bpy/Pt/bpy)_5$ films is uniform and the mean size of NPs is 3.79 nm after the 10th cycle of styrene hydrogenation (Figure 7). When the reaction reacted for a long time, NPs tend to aggregate after the 10th cycle of nitrobenzene hydrogenation (Figure 8). However, the mean size of NPs still remains small (5.46 nm). Small sizes of NPs results in high catalytic activity after recyling for many times.

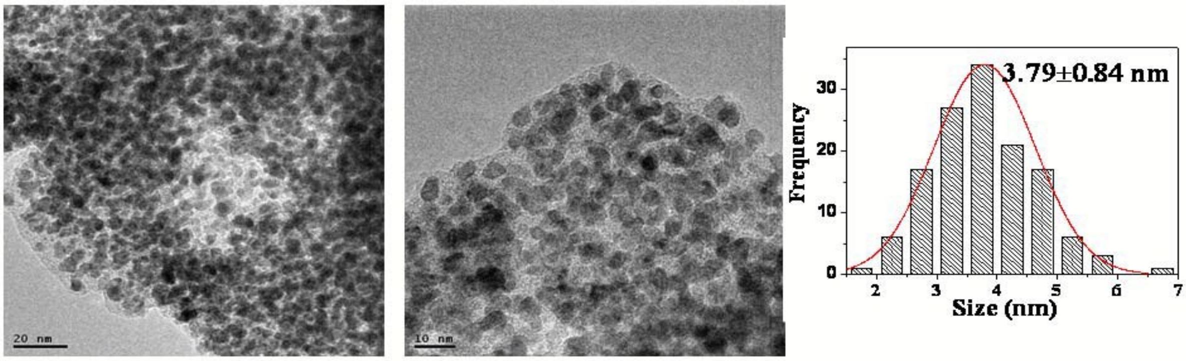

Fig.7 TEM images of (Pd/bpy/Pt/bpy)$_5$ films after the 10th cycle of styrene hydrogenation

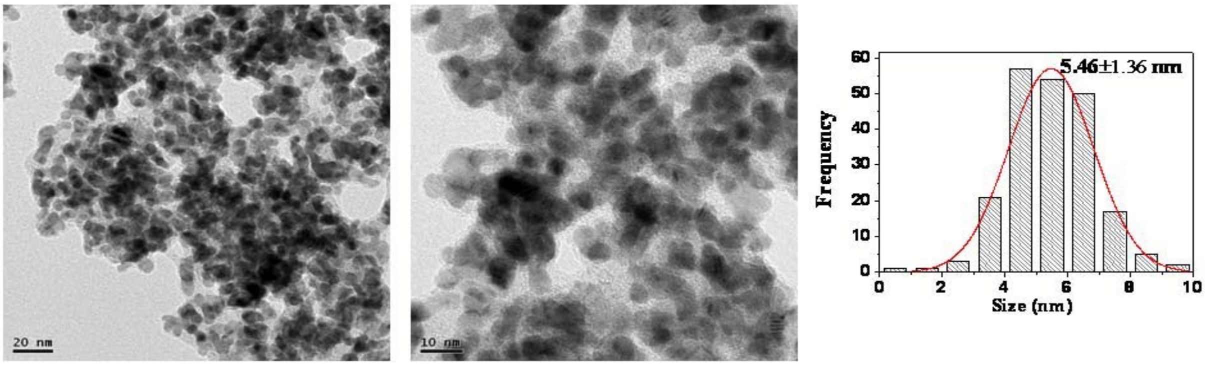

Fig.8 TEM images of (Pd/bpy/Pt/bpy)$_5$ films after the 10th cycle of nitrobenzene hydrogenation

In order to confirm the high catalytic activity of the catalyst, the control experiments using the prereduced (Pd/bpy/Pt/bpy)$_5$ bimetallic catalyst (H_2 reduction at 150 ℃) and the physical mixtures of the Pd and Pt film catalysts were performed. The results are shown in Table 2. TOF (moles of substrate converted per mole of catalyst per h) of (Pd/bpy)$_5$ and (Pt/bpy)$_5$ mixed films catalysts is 295 h^{-1} (Table 2, entry 1), while TOF of the prereduced (Pd/bpy/Pt/bpy)$_5$ bimetallic catalyst is 378 h^{-1} (Table 2, entry 2). The *in situ* reduced (Pd/bpy/Pt/bpy)$_5$ film catalyst has the highest TOF of 669 h^{-1} (Table 2, entry 3). This may be explained as following: Metal ions are gradually reduced into NPs for bimetallic films, but Pt(II) ions are more difficult reduced than Pd(II) ions under the same condition. Therefore, the catalytic activity of bimetallic (Pd/bpy/Pt/bpy)$_5$ films comes from Pd NPs firstly. With the reaction going on, the reduced Pt NPs appeared and the synergistic action of bimetallic Pd/Pt might enhance the catalytic activity.[28, 29] Moreover, the internal structure of the bimetallic complex films may have an effect on the catalytic activtiy. The terminal pyridyl group of bpy is coordinated to Pd ions, while the other pyridyl group is connected with Pt ion.

Table 2 Hydrogenation of nitrobenzene over different film catalysts

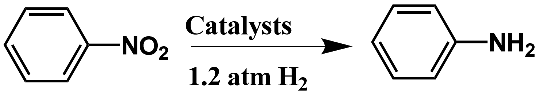

Entry	Catalysts	Pd (mol) ×10^{-7}	Pt (mol) ×10^{-8}	Yield (%)^a	TOF (h^{-1})
1	(Pd/bpy)$_5$ film and (Pt/bpy)$_5$ film	1.9	1.3	24	295
2	(Pd/bpy/Pt/bpy)$_5$ film (prereduced)	2.0	8.4	43	378
3	(Pd/bpy/Pt/bpy)$_5$ film	2.0	8.4	76	669

Reaction conditions: 0.5 mmol of nitrobenzene, absolute ethanol (10 ml), stirring, H_2 (1.2 atm), 34℃, time (2.0 h), TOF (moles of substrate converted per mole of catalyst per h), ^{a} Determined by GC methods.

Thus, Pd NPs of bimetallic films cannot easily tend to aggregate compared with monometallic films, resulting high catalytic activity.

Conclusions

In the present work, bimetallic layer-by-layer catalytic $(Pd/bpy/Pt/bpy)_n$ films were first successfully prepared. The bimetallic-pyridyl catalytic films exhibit a superior catalytic activity toward hydrogenation of olefin under mild conditions. In view of activity, $(Pd/bpy/Pt/bpy)_5$ films exhibit better performance than that of monometallic film counterparts.[25] The results of XPS and TEM results also further demonstrated that Pd(II) and Pt(II)ions of bimetallic films were gradually *in situ* converted to NPs, resulting in the higher activity. The control experiments further indicate that *in situ* reduced into Pd and Pt nanoparticles and the synergistic action of bimetallic Pd/Pt result in higher catalytic activity. Moreover, our bimetallic catalytic films have the superiority compared with traditional heterogeneous catalysts, due to high efficiency, ease of catalyst separation and good recyclability.

Acknowledgements

This work was financially supported by 973 Program (2011CB932504 and 2012CB821705), NSFC (21331006, 21173222 and 21221001), the ‘‘Strategic Priority Research Program’’ of the Chinese Academy of Sciences (XDA09030102), the Key Project from CAS.

Notes and references

[a] *State Key Laboratory of Structural Chemistry, Fujian Institute of Research on the Structure of Matter, the Chinese Academy of Sciences, Fuzhou 350002, China. E-mail：rcao@fjirsm.ac.cn*

1 S. Hirasawa, H. Watanabe, T. Kizuka, Y. Nakagawa and K. Tomishige, *J. Catal., 2*013, **300,** 205.
2 W. G. Menezes, L. Altmann, V. Zielasek, K. Thiel and M. Bäumer, *J. Catal.*, 2013, **300,** 125.
3 Z. Wei, J. Sun, Y. Li, A. K. Datyec and Y. Wang, *Chem. Soc. Rev.*, 2012, **41,** 7994.
4 W. Yu, M. D. Porosoff and J. G. Chen, *Chem. Rev.,* 2012, **112,** 5780.
5 Y. Xiang, S. Lu and S. P. Jiang, *Chem. Soc. Rev.*, 2012, **41,** 7291.
6 H. Xu, W. Cao and X. Zhang, *Accounts Chem. Res.*, 2013, **46,** 1647.
7 M. Yang, S. Lu, J. Lu, S. P. Jiang and Y. Xiang, *Chem. Commun.*, **2010,** 1434.
8 A. Zhuk and S. A. Sukhishvili, *Soft Matter,* 2013, **9,** 5149.
9 A. Mentbayeva, A. Ospanova, Z. Tashmuhambetova, V. Sokolova and S. Sukhishvili, *Langmuir,* 2012, **28,** 11948.
10 S. Kidambi, J. Dai, J. Li and M. L. Bruening, *J. Am. Chem. Soc.*, 2004, **126,** 2658.
11 S. Kidambi and M.L. Bruening, *Chem. Mater.*, 2005, **17,** 301.
12 S. Bhattacharjee and M. L. Bruening, *Langmuir,*2008, **24,** 2916.
13 Y. Wang and J-K Lee, *J. Mol. Catal. A: Chem.,* 2007, **263,** 163.
14 Z. Ren, H.-L. Wang, Y.-Q. Cai, M. Chen and D-J Qian, *Mater. Chem. Phys.,* 2011, **127,** 310.
15 M. Altman, A. D. Shukla, T. Zubkov, G. Evmenenko, P. Dutta and M. E. van der Boom, *J. Am. Chem. Soc.*, 2006, **128,** 7374.
16 M. Altman, O. V. Zenkina, T. Ichiki, M. A. Iron, G. Evmenenko, P. Dutta and M. E. van der Boom, *Chem. Mater.*, 2009, **21,** 4676.
17 J. Choudhury, R. Kaminker, L. Motiei, G. de Ruiter, M. Morozov, F. Lupo, A.Guilino and M. E. van der Boom, *J. Am. Chem. Soc.,* 2010, **132,** 9295.
18 T. N. Milie, N. Chi, D. G.Yablon, G. W. Flynn, J. D. Batteas and C. M. Drain, *Angew. Chem. Int. Ed.,* 2002, **41,** 2117.
19 T. Milic, J. C. Garno, J. D. Batteas, G. Smeureanu and C. M. Drain, *Langmuir,* 2004, **20,** 3974.
20 S. Gao, Z. Zheng , J. Lü and R. Cao, *Chem. Commun.,* 2010, **46，** 7584.
21 L. Zhang, C. Wang and Y. Zhang, *Appl. Surface Sci.*, 2012, **258,** 5312.
22 L. Shang, L. Jin, S. Guo, J. Zhai and S. Dong, *Langmuir,* 2010, **26,** 6713.
23 X. Liu, A. Wang, X. Yang, T. Zhang, C.-Y. Mou, D.-S. Su and J. Li, *Chem. Mater.*, 2009, **21,** 410.
24 X. Zhang and Z. Su, *Adv. Mater.,* 2012, **24,** 4574.
25 S. Gao, M. Cao, W. Li and R. Cao, *J. Mater. Chem. A,* 2014, **2,** 12185.
26 S. Kidambi and M. L. Bruening, *Chem. Mater.*, 2005, **17,** 301.
27 C. Dablemont, P. Lang, C. Mangeney, J.-Y. Piquemal, V. Petkov, F. Herbst and G. Viau, *Langmuir,* 2008, **24,** 5832.
28 R. W. J. Scott, A. K. Datye and R. M. Crooks, *J. Am. Chem. Soc.*, 2003, **125,** 3708.
29 B. A. Kakade, T. Tamaki, H. Ohashi and T. Yamaguchi, *J. Phys. Chem. C,* 2012, **116,** 7464.